JOURNAL OF CHEMICAL INFORMATION AND MODELING

pubs.acs.org/jcim

Application Note

CHARMM-GUI Free Energy Calculator for Practical Ligand Binding Free Energy Simulations with AMBER

Han Zhang, Seonghoon Kim, Timothy J. Giese, Tai-Sung Lee, Jumin Lee, Darrin M. York, and Wonpil Im*

Cite This: J. Chem. Inf. Model. 2021, 61, 4145−4151

Read Online

ACCESS | Metrics & More | Article Recommendations | Supporting Information

ABSTRACT: Alchemical free energy methods, such as free energy perturbation (FEP) and thermodynamic integration (TI), become increasingly popular and crucial for drug design and discovery. However, the system preparation of alchemical free energy simulation is an error-prone, time-consuming, and tedious process for a large number of ligands. To address this issue, we have recently presented CHARMM-GUI *Free Energy Calculator* that can provide input and postprocessing scripts for NAMD and GENESIS FEP molecular dynamics systems. In this work, we extended three submodules of *Free Energy Calculator* to work with the full suite of GPU-accelerated alchemical free energy methods and tools in AMBER, including input and postprocessing scripts. The BACE1 (β-secretase 1) benchmark set was used to validate the AMBER-TI simulation systems and scripts generated by *Free Energy Calculator*. The overall results of relatively large and diverse systems are almost equivalent with different protocols (unified and split) and with different timesteps (1, 2, and 4 fs), with $R^2 > 0.9$. More importantly, the average free energy differences between two protocols are small and reliable with four independent runs, with a mean unsigned error (MUE) below 0.4 kcal/mol. Running at least four independent runs for each pair with AMBER20 (and FF19SB/GAFF2.1/OPC force fields), we obtained a MUE of 0.99 kcal/mol and root-mean-square error of 1.31 kcal/mol for 58 alchemical transformations in comparison with experimental data. In addition, a set of ligands for T4-lysozyme was used to further validate our free energy calculation protocol whose results are close to experimental data (within 1 kcal/mol). In summary, *Free Energy Calculator* provides a user-friendly web-based tool to generate the AMBER-TI system and input files for high-throughput binding free energy calculations with access to the full set of GPU-accelerated alchemical free energy, enhanced sampling, and analysis methods in AMBER.

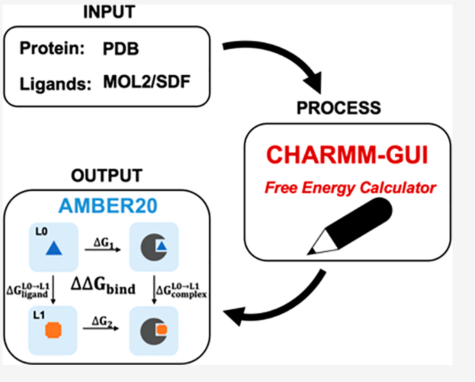

INTRODUCTION

Alchemical free energy calculations are widely used for computer-aided drug design and discovery.[1−8] Free energy perturbation (FEP) and thermodynamic integration (TI) are the two most popular alchemical methods that show promising results with high accuracy for the absolute and relative binding free energy prediction. Both methods are implemented in various molecular dynamics (MD) simulation program packages, such as NAMD,[9−11] AMBER,[12−15] GROMACS,[16,17] CHARMM,[18] and GENESIS.[19]

In particular, since the 1980s, AMBER has supported alchemical free energy simulation and has been used for drug design research for decades. AMBER supports both absolute and relative binding free energy calculations. Recently, relative binding free energy ($\Delta\Delta G_{bind}$) calculations have drawn increasing attention, as they require less computational resources than absolute binding free energy calculations.[9,20−22] These calculations have become practical with high performance implementation on graphical processing units (GPUs).[23−25] The advances in AMBER20 provide further improved reliability and simulation speed of protein−ligand $\Delta\Delta G_{bind}$ calculations.[13]

The system preparation of alchemical free energy simulation is an error-prone, time-consuming, and tedious process for a large number of ligands. Therefore, the implementation of user-friendly computational tools to automatize sophisticated system building and input generation is critical and essential for drug design and discovery research. CHARMM-GUI[26] (https://www.charmm-gui.org) is a widely used web-based platform that provides a well-designed workflow to generate complex molecular simulation system and input scripts.[27−39] The *Free Energy Calculator* module includes four submodules (*Absolute Ligand Solvator*, *Absolute Ligand Binder*, *Relative Ligand Solvator*, and *Relative Ligand Binder*) to help researchers

Received: June 26, 2021
Published: September 15, 2021

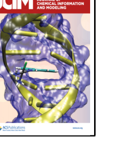

https://doi.org/10.1021/acs.jcim.1c00747
J. Chem. Inf. Model. 2021, 61, 4145−4151

set up FEP/MD simulation systems and input scripts for CHARMM, NAMD, and GENESIS.[39,40] In this work, we present its extension to support an AMBER GPU-accelerated alchemical free energy simulation system setup and input generation for *Absolute Ligand Solvator*, *Relative Ligand Solvator*, and *Relative Ligand Binder*. In particular, CHARMM-GUI provides various AMBER force field (FF) combinations for researchers to choose based on their preference and need. In addition, *Free Energy Calculator* supports hydrogen mass repartitioning (HMR) as an option to increase a time step to 4 fs for accelerated AMBER-TI simulations.[41,42]

This study aims to illustrate how *Free Energy Calculator* can be used for practical ligand binding AMBER-TI simulations with AMBER20. For this, we performed AMBER-TI simulations for the BACE1 (β-secretase 1) benchmark set using different timesteps (1, 2, and 4 fs) and protocols (unified and split).[13,43] In the split (or stepwise or multistep) protocol, there are "decharge-vdW-recharge" three steps in which Coulombic electrostatic and van der Waals (vdW) interactions are scaled separately. For the unified (or concerted or one-step) protocol, both electrostatic and vdW interactions are scaled concurrently by the softcore potentials.[44] Our results indicate that running multiple (at least 4) independent runs is crucial and essential to get reasonable, stable, and reliable free energy results regardless of timesteps. In addition, with four independent runs, both unified and split protocols yield almost equivalent results. Therefore, one could obtain reliable $\Delta\Delta G_{\mathrm{bind}}$ by performing at least 4 AMBER-TI runs using the unified protocol and 4 fs time step with HMR.

■ METHODS

Amber-TI System and Input Generation in *Free Energy Calculator*. *Free Energy Calculator* consists of four submodules and is designed to support various ligand solvation and binding free energy calculations: *Absolute Ligand Solvator* (*ALS*), *Absolute Ligand Binder* (*ALB*), *Relative Ligand Solvator* (*RLS*), and *Relative Ligand Binder* (*RLB*). The detailed workflow has been introduced in our recent work.[39] Here, we present an extension of *ALS*, *RLS*, and *RLB* submodules to support an AMBER GPU-accelerated alchemical free energy simulation system and input generation. The overall workflow for the AMBER system setup is the same as for the NAMD and GENESIS FEP/MD setup, except for the FF selection part. Currently, AMBER-TI is only compatible with the AMBER FFs. As shown in Figure 1A, CHARMM-GUI supports various AMBER FFs: FF14SB[45] and FF19SB[46] for protein, general AMBER force field (GAFF)[47] and GAFF2.1[48] for ligand, and TIP3P,[49] TIP4PEW,[50] TIP4PD,[51] and OPC[52] for water; in this work, we do not discuss DNA, RNA, glycan, and lipid FFs, although they are supported. There are 16 different FF combinations if we consider a protein−ligand complex system with the different water models, and researchers can choose any FF combination based on their preference and research need. *Free Energy Calculator* checks if a given ligand set can be parametrized by GAFF or GAFF2.1 successfully, and the pair containing any ligand that is not supported by the selected ligand FF needs to be removed (Figure 1B). In addition, HMR is supported as an option to allow a simulation time step of 4 fs (Figure 1A). We will present two systems in the main manuscript, but multiple challenging systems (Figure S1) were successfully prepared via *Free Energy Calculator* (see the Supporting Information for more details).

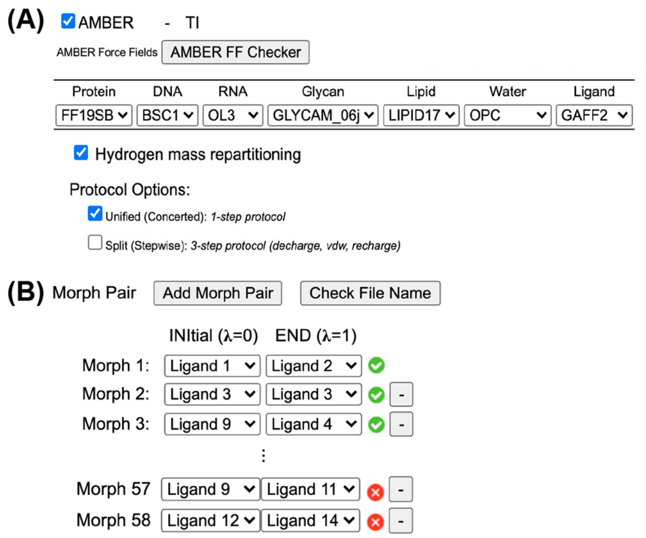

Figure 1. (A) AMBER FF selection in *Free Energy Calculator*. (B) Snapshot after clicking AMBER FF Checker, and the pair containing any ligand that is not supported by the selected ligand FF is marked as an error flag in red.

System Setup and Protocols. BACE1 (PDB 4DJW) was used to validate the generated AMBER-TI systems and inputs from *Free Energy Calculator*. As shown in Table S1, 36 ligands[53] were used to generate 58 pairs[54] in the BACE1 benchmark set. Based on the uploaded ligand structure files (MOL2 or SDF), *Free Energy Calculator* determines the common and unique atoms using a maximum common structure algorithm.[55,56] The common atoms of ligand 0 (L0) and ligand 1 (L1) have the same coordinates. In each alchemical transformation system, the unique atoms are in the softcore regions. The atoms in the softcore regions of L0 and L1 are defined as "scmask1" and "scmask2", respectively. As shown in Figure S2, for example, the softcore regions of pair CAT-13a ("scmask1") to CAT-17g ("scmask2") are highlighted by red and blue dashed rectangles, respectively. Each pair system was generated with the unified protocol in which both electrostatic and vdW interactions are scaled concurrently by the softcore potentials. Fifteen pairs were randomly selected to compare the results from the unified protocol with those from the split protocol in which electrostatic and vdW interactions are scaled separately. In the split protocol, the atoms in the softcore region (i.e., the atoms that will be transformed into dummy atoms) are decharged first. Then, the decharged atoms go through the vdW transformation via the softcore potential. Finally, the atoms in the softcore region are recharged to the end state.

An accurate FF is crucial for reliable $\Delta\Delta G_{\mathrm{bind}}$ prediction. FF19SB shows improved backbone profiles for all 20 amino acid residues, and the OPC water model is recommended when it is used.[46] In this study, the protein, water, and ligands were modeled with the FF19SB, OPC, and GAFF2.1 FFs, respectively. All simulation systems were solvated in a cubic water box consisting of water molecules and neutralized by counterions (KCl).

A thermodynamic cycle for $\Delta\Delta G_{\mathrm{bind}}$ calculation is shown in Figure S3. $\Delta\Delta G_{\mathrm{bind}}$ between L0 and L1 ligands in the same target protein is calculated by

$$\Delta\Delta G_{\mathrm{bind}}^{\mathrm{L0}\rightarrow\mathrm{L1}} = \Delta G_{\mathrm{complex}}^{\mathrm{L0}\rightarrow\mathrm{L1}} - \Delta G_{\mathrm{ligand}}^{\mathrm{L0}\rightarrow\mathrm{L1}} \quad (1)$$

https://doi.org/10.1021/acs.jcim.1c00747
J. Chem. Inf. Model. 2021, 61, 4145−4151

where $\Delta G_{\text{complex}}^{\text{L0}\rightarrow\text{L1}}$ and $\Delta G_{\text{ligand}}^{\text{L0}\rightarrow\text{L1}}$ are the alchemical transformations of L0 to L1 in the complex and solution, respectively. The free energy difference between states L0 and L1 can be calculated as

$$\Delta G_{\text{complex/ligand}}^{\text{L0}\rightarrow\text{L1}} = \int_0^1 \left\langle \frac{\partial U(\lambda)}{\partial \lambda} \right\rangle \mathrm{d}\lambda \tag{2}$$

where $U(\lambda)$ is the λ-coupled potential energy and λ is a coupling parameter varying from 0 (L0) to 1 (L1). The integration is calculated via the average of the λ derivative of the coupled potential energy at each intermediate λ state. The ΔG values are obtained by the sum of numerical integration over N (the number of λ windows) quadrature points with associated weights of $\partial U/\partial\lambda$. In this work, 21 λ windows (λ value from 0 to 1 with $\Delta\lambda$ = 0.05) were applied for each complex system and solution system. Long-range electrostatics in solution was treated with the particle mesh Ewald (PME) method, and the vdW interactions were calculated with a cutoff distance of 10 Å.[57,58] The second-order smoothstep softcore potential, SSC(2), was applied in the simulation.[13] The values of 0.2 and 50 Å^2 were used for the parameters α and β of the softcore potential, respectively. Equilibration was performed for 5 ps employing the NPT (constant particle number, pressure, and temperature) ensemble after minimization in each λ window. AMBER-TI simulations were performed in the NPT ensemble at 300 K and 1 atm (1.0135 bar) with the pmemd.cuda module of AMBER20. All 58 alchemical transformations were run with a 4 fs time step with HMR using the unified protocol. The randomly selected 15 pairs were additionally run with a 1 fs time step and a 2 fs time step without HMR and a 4 fs time step with HMR using both the unified and split protocols. For each λ of all $\Delta\Delta G_{\text{bind}}$ calculations, 5 ns AMBER-TI simulations were performed, and the last 4 ns of the simulations results were utilized for the final $\Delta\Delta G_{\text{bind}}$ values.

■ RESULTS AND DISCUSSION

Overall Performance of Three Different Timesteps. We randomly selected 15 pairs out of 58 pairs in the BACE1 benchmark set to run AMBER-TI simulations with both unified and split protocols and with 1, 2, and 4 fs timesteps. For 1 and 2 fs simulations, we ran four independent runs for each alchemical transformation. HMR was used for 4 fs time step simulations, and we ran eight independent runs for each pair. Figure 2 shows the comparison of the $\Delta\Delta G_{\text{bind}}$ results using different timesteps within the unified and split protocols. All R^2 values between the systems with different timesteps are larger than 0.9, indicating consistent $\Delta\Delta G_{\text{bind}}$ prediction with different timesteps within the same protocol. Note that it is possible that one cannot perform AMBER-TI simulations with a 4 fs time step and SHAKE. For instance, based on our experience, for the transformation having X−C−H and X−N atoms, when X−C and X−N atoms are defined as the common region and the H atom is defined as a softcore atom, a 4 fs time step and SHAKE could be problematic. In such cases, one may need to use a 1 fs time step without SHAKE to perform the AMBER-TI simulations.[43]

Overall Performance of the Unified and Split Protocols. To compare the results between two different protocols, for the randomly selected 15 pairs, we calculated the mean unsigned error (MUE) ($|\Delta\Delta G_{\text{unified}} - \Delta\Delta G_{\text{split}}|$) between the unified and split protocols as a function of number of independent runs. For 1 and 2 fs time step simulations, 16, 36, 16, and 1 different cases need to be compared for 1, 2, 3, and 4 independent runs, respectively. Similarly, for 4 fs time step simulations, 64, 784, 3136, 4900, 3136, 784, 64, and 1 different cases need to be compared for 1, 2, 3, 4, 5, 6, 7, and 8 independent runs, respectively. The box plots in Figure 3A−C display the distributions of data into quartiles for a given set of values and 75% of the values fall below the upper quartile. The median, middle quartile, marks the midpoint of the data and is shown by a line in the box. The middle box represents the middle 50% of the values for the group. Figure 3A,B show the MUE of $\Delta\Delta G_{\text{bind}}$ between the unified and split protocols for 1 and 2 fs simulations. Both 1 and 2 fs simulations show similar results, and the $\Delta\Delta G_{\text{bind}}$ differences become smaller with more independent runs, with a MUE value below 0.45 kcal/mol with four independent runs. Figure 3C shows the comparison for the results of 4 fs simulations. The MUE between two protocols becomes converged after four independent runs with a MUE value below 0.40 kcal/mol. Even with more number of independent runs, the MUE value is kept almost unchanged, which is always between 0.35 and 0.40 kcal/mol after four independent runs. Our results indicate that multiple independent runs, at least four, are required and necessary to get statistically consistent $\Delta\Delta G_{\text{bind}}$ from the unified and split protocols in AMBER-TI. In addition, Figure 3D shows a high correlation of calculated $\Delta\Delta G_{\text{bind}}$ between the unified and split protocols for three different timesteps. The overall performance of the unified and split protocol is almost equivalent. Therefore, the unified

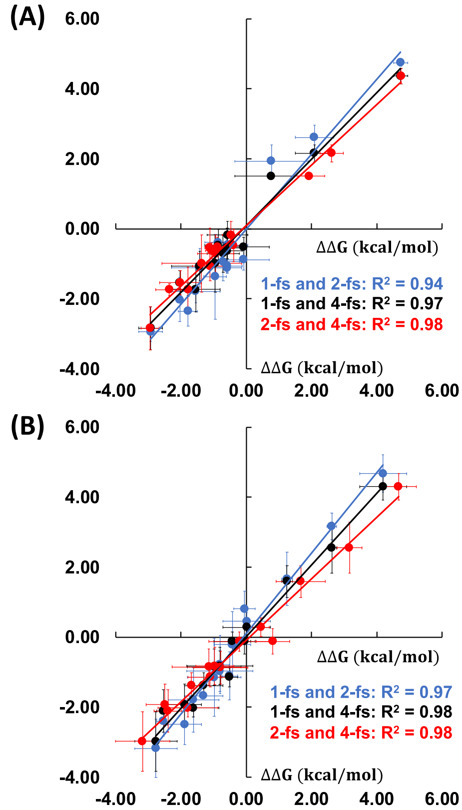

Figure 2. Comparison of 15 $\Delta\Delta G_{\text{bind}}$ values using different timesteps with the (A) unified and (B) split protocols. Comparisons between 1 and 2 fs timesteps, 1 and 4 fs timesteps, and 2 and 4 fs timesteps are shown by blue, black, and red dots with each least-square fit line, respectively.

https://doi.org/10.1021/acs.jcim.1c00747
J. Chem. Inf. Model. 2021, 61, 4145−4151

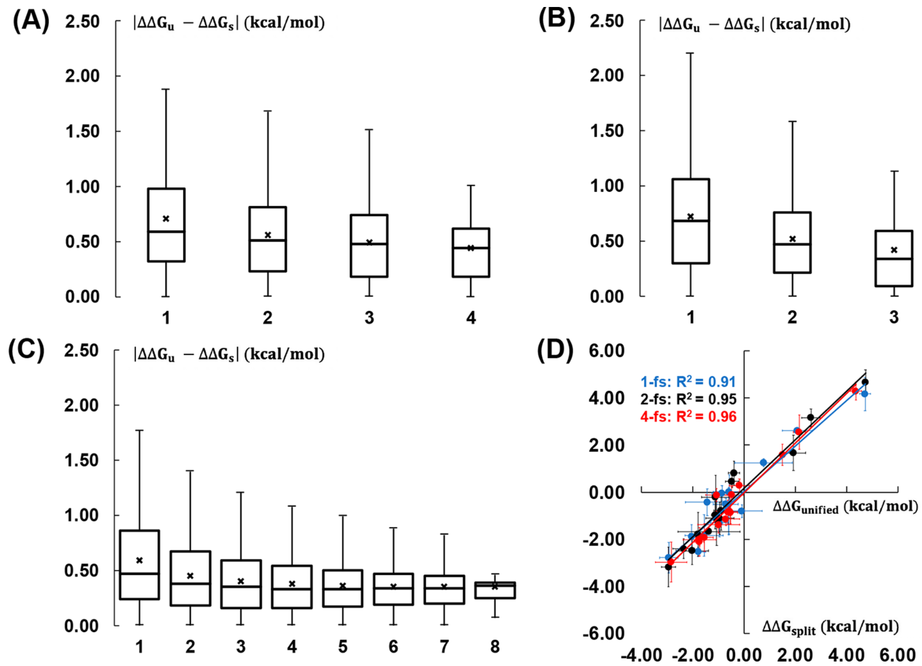

Figure 3. Mean unsigned energy differences between the unified and split protocols for the AMBER-TI simulations with (A) 1 fs, (B) 2 fs, and (C) 4 fs timesteps. The *X*-axis is the number of independent runs that are considered for the comparison. The × mark represents the average value of each comparison. All the outliers are not shown in the box and whisker plots. (D) Correlation between $\Delta\Delta G_{\mathrm{bind}}$ from the unified and split protocols. $\Delta\Delta G_{\mathrm{bind}}$ calculations with 1, 2, and 4 fs timesteps are in blue, black, and red, respectively.

protocol using a 4 fs time step with HMR is recommended for practical $\Delta\Delta G_{\mathrm{bind}}$ prediction from the resource consumption perspective.

Comparison between Calculated and Experimental $\Delta\Delta G_{\mathrm{bind}}$. We ran AMBER-TI simulations with 4 independent runs for the remaining 43 pairs out of 58 alchemical transformations in the BACE1 benchmark set with the unified protocol and 4 fs time step. Figure 4A shows the comparison between experimental and our calculated $\Delta\Delta G_{\mathrm{bind}}$ values for 58 pairs. The MUE and root-mean-square error (RMSE) of the $\Delta\Delta G_{\mathrm{bind}}$ values compared to the experimental data are 0.99 and 1.39 kcal/mol, respectively (Table 1). We predicted the absolute binding free energy (ΔG_{bind}) for all 36 ligands in the BACE1 system by following the method described previously[54] and compared the results to experimental data (Figure 4B). The R^2 is 0.28 and three of 36 ligands deviate from their experimental free energies by more than 2 kcal/mol. The three ligands are CAT-17a, CAT-4d, and CAT-4l, and the deviations from ΔG_{exp} are 2.07, 2.21, and 2.44 kcal/mol, respectively. Overall, as shown in Table 1, our calculations show comparable results with a previous AMBER-TI study, and both AMBER-TI results are worse than the FEP+ results.

We implemented the cycle closure convergence strategy described previously[59] to get another predicted $\Delta\Delta G_{\mathrm{bind}}$. The R^2 between these predicted ΔG_{bind} and experimental data is not improved. However, as shown in the black dots in Figure 4B, only one ligand deviates from their experimental free energies by more than 2 kcal/mol after the cycle closure convergence. The deviation from ΔG_{exp} of ligand CAT-17a and CAT-4d are improved to 0.88 and 1.84 kcal/mol, respectively, but the deviation of CAT-4l becomes 2.60 kcal/mol.

T4-Lysozyme Test Systems. To further validate the systems generated by *Relative Ligand Binder*, we tested three different alchemical transformations in T4-lysozyme (Figure

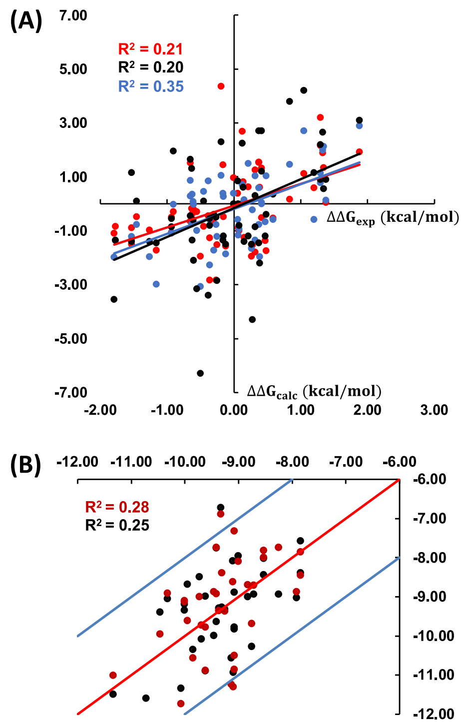

Figure 4. (A) Correlation between calculated $\Delta\Delta G_{\mathrm{bind}}$ and experimental data for 58 pairs in the BACE1 benchmark set. The correlation for AMBER20, AMBER18,[14] and FEP+[54] are in red, black, and blue, respectively. (B) Correlation between predicted ΔG_{bind} and experimental results for 36 ligands in the BACE1 system for AMBER20 is in red, and the correlation between another predicted ΔG_{bind} (after the cycle closure convergence) and experimental results is in black. The *X*-axis and *Y*-axis are the experimental and predicted ΔG_{bind} (kcal/mol), respectively.

https://doi.org/10.1021/acs.jcim.1c00747
J. Chem. Inf. Model. 2021, 61, 4145−4151

Table 1. Statistics of $\Delta\Delta G_{bind}$ Comparisons with the Experimental Data

force field	R^2	MUE (kcal/mol)	RMSE (kcal/mol)
FF-1[a]	0.21	0.99	1.31
FF-2[b]	0.20	1.33	1.79
FF-3[c]	0.35	0.87	1.05

[a]AMBER-TI FF19SB + GAFF2.1 + OPC. [b]AMBER-TI FF14SB + GAFF1.8 + SPC/E.[14] [c]FEP+/OPLS 2.1 + SPC.[54]

S4). Four AMBER-TI runs were performed for each pair, and results are shown in Table 2. The calculated $\Delta\Delta G_{bind}$ of three alchemical transformations are comparable with the previous calculations based on NAMD and GENESIS as well as the experimental data within 1 kcal/mol. The standard errors of predicted $\Delta\Delta G_{bind}$ are below 0.15 kcal/mol and are omitted in Table 2.

Table 2. $\Delta\Delta G_{bind}$ Results (kcal/mol) of Three Alchemical Transformations of T4-Lysozyme in Figure S4A

ligand 0	tol[b]		
ligand 1	Bz[b]	EB[b]	PB[b]
$\Delta\Delta G_{exp}$	0.33	−0.24	−1.03
$\Delta\Delta G_{NAMD}$[a]	−0.23	−0.66	−2.14
$\Delta\Delta G_{GENESIS}$[a]	−0.10	−0.43	−1.57
$\Delta\Delta G_{AMBER\text{-}TI}^{unified}$	−0.27	−0.90	−1.68

[a]$\Delta\Delta G_{bind}$ results using NAMD and GENESIS are from Kim et al.[39] [b]tol, Bz, EB, and PB are the abbreviations of toluene, benzene, ethylbenzene, and propylbenzene, respectively.

CONCLUSIONS

In this work, we have presented an extension of CHARMM-GUI *Free Energy Calculator* to support the full suite of GPU-accelerated alchemical free energy methods and tools in AMBER together with two benchmark testing sets. Such an extension provides a user-friendly web-based tool to generate an AMBER-TI system and input files for practical throughput binding free energy calculations. The CHARMM-GUI interface allows users to select various options, including the use of HMR and the choice of protein, water, and ligand FFs.

BACE1 and T4-lysozyme benchmark sets were used to validate the AMBER-TI systems and input scripts generated from *Free Energy Calculator* by calculating $\Delta\Delta G_{bind}$ with multiple independent runs. In particular, with randomly selected 15 pairs in the BACE1 benchmark set, our results show that the overall performance of the unified and split protocols is very similar regardless of the timesteps (1, 2, or 4 fs). In addition, our results indicate that multiple independent runs are required and necessary to calculate statistically reliable $\Delta\Delta G_{bind}$ using AMBER-TI. Based on our results, our recommendation is to perform at least 4 AMBER-TI runs using the unified protocol and 4 fs time step with HMR for practical throughput $\Delta\Delta G_{bind}$ calculations. Additional independent runs might be required for more complicated protein–ligand systems. Therefore, users need to decide the number of independent runs for their own systems based on their understanding of the specific proteins.

The overall $\Delta\Delta G_{bind}$ values with a FF19SB + GAFF2.1 + OPC FF combination in this study are slightly better than those with the FF14SB + GAFF1.8 + SPC/E FF combination[14] for the same set of ligands. This indicates that with the robust AMBER-TI calculations, better FFs would yield better predictions. In this context, our ongoing efforts are to check all AMBER FF combinations in $\Delta\Delta G_{bind}$ calculations and their dependence on the number of λ windows and simulation time.

ASSOCIATED CONTENT

Supporting Information

The Supporting Information is available free of charge at https://pubs.acs.org/doi/10.1021/acs.jcim.1c00747.

Table S1, 58 $\Delta\Delta G_{bind}$ pathways for 36 ligands; detailed $\Delta\Delta G_{bind}$ values with unified and split protocols and with three timesteps; MUE and RMSE calculations; and ΔG_{bind} calculations (PDF)

Experimental $\Delta\Delta G_{bind}$ values (XLSX)

AUTHOR INFORMATION

Corresponding Author

Wonpil Im − *Department of Biological Sciences, Chemistry, Bioengineering, and Computer Science and Engineering, Lehigh University, Pennsylvania 18015, United States;* orcid.org/0000-0001-5642-6041; Email: wonpil@lehigh.edu

Authors

Han Zhang − *Department of Biological Sciences, Chemistry, Bioengineering, and Computer Science and Engineering, Lehigh University, Pennsylvania 18015, United States;* orcid.org/0000-0002-5608-9185

Seonghoon Kim − *School of Computational Sciences, Korea Institute for Advanced Study, Seoul 02455, Republic of Korea;* orcid.org/0000-0002-0050-1054

Timothy J. Giese − *Laboratory for Biomolecular Simulation Research, Institute for Quantitative Biomedicine, and Department of Chemistry and Chemical Biology, Rutgers, the State University of New Jersey, New Jersey 08854, United States;* orcid.org/0000-0002-0653-9168

Tai-Sung Lee − *Laboratory for Biomolecular Simulation Research, Institute for Quantitative Biomedicine, and Department of Chemistry and Chemical Biology, Rutgers, the State University of New Jersey, New Jersey 08854, United States;* orcid.org/0000-0003-2110-2279

Jumin Lee − *Department of Biological Sciences, Chemistry, Bioengineering, and Computer Science and Engineering, Lehigh University, Pennsylvania 18015, United States;* orcid.org/0000-0002-1008-0118

Darrin M. York − *Laboratory for Biomolecular Simulation Research, Institute for Quantitative Biomedicine, and Department of Chemistry and Chemical Biology, Rutgers, the State University of New Jersey, New Jersey 08854, United States;* orcid.org/0000-0002-9193-7055

Complete contact information is available at: https://pubs.acs.org/10.1021/acs.jcim.1c00747

Notes

The authors declare no competing financial interest.

Data and Software Availability. All the protein structures and molecular dynamics data are available upon request. *Free Energy Calculator* module can be accessed through the following link: https://www.charmm-gui.org/input/fec.

■ ACKNOWLEDGMENTS

This work was supported in part by the grants from NIH Grant GM138472 (W.I.) and NIH Grants GM107485 and GM062248 (D.M.Y.). We thank Hsu-Chun Tsai, Yujun Tao, and Abir Ganguly for their helpful discussion on AMBER-TI inputs.

■ REFERENCES

(1) Gilson, M. K.; Given, J. A.; Bush, B. L.; McCammon, J. A. The statistical-thermodynamic basis for computation of binding affinities: a critical review. *Biophys. J.* **1997**, *72* (3), 1047−69.

(2) Jorgensen, W. L. The many roles of computation in drug discovery. *Science* **2004**, *303* (5665), 1813−8.

(3) Jorgensen, W. L. Efficient drug lead discovery and optimization. *Acc. Chem. Res.* **2009**, *42* (6), 724−33.

(4) Gilson, M. K.; Zhou, H. X. Calculation of protein-ligand binding affinities. *Annu. Rev. Biophys. Biomol. Struct.* **2007**, *36*, 21−42.

(5) Mobley, D. L.; Dill, K. A. Binding of small-molecule ligands to proteins: "what you see" is not always "what you get. *Structure* **2009**, *17* (4), 489−98.

(6) Chodera, J. D.; Mobley, D. L.; Shirts, M. R.; Dixon, R. W.; Branson, K.; Pande, V. S. Alchemical free energy methods for drug discovery: progress and challenges. *Curr. Opin. Struct. Biol.* **2011**, *21* (2), 150−60.

(7) Shirts, M. R. Best practices in free energy calculations for drug design. *Methods Mol. Biol.* **2012**, *819*, 425−67.

(8) Jespers, W.; Aqvist, J.; Gutierrez-de-Teran, H. Free Energy Calculations for Protein-Ligand Binding Prediction. *Methods Mol. Biol.* **2021**, *2266*, 203−226.

(9) Jiang, W.; Chipot, C.; Roux, B. Computing Relative Binding Affinity of Ligands to Receptor: An Effective Hybrid Single-Dual-Topology Free-Energy Perturbation Approach in NAMD. *J. Chem. Inf. Model.* **2019**, *59* (9), 3794−3802.

(10) Chatterjee, P.; Botello-Smith, W. M.; Zhang, H.; Qian, L.; Alsamarah, A.; Kent, D.; Lacroix, J. J.; Baudry, M.; Luo, Y. Can Relative Binding Free Energy Predict Selectivity of Reversible Covalent Inhibitors? *J. Am. Chem. Soc.* **2017**, *139* (49), 17945−17952.

(11) Zhang, H.; Jiang, W.; Chatterjee, P.; Luo, Y. Ranking Reversible Covalent Drugs: From Free Energy Perturbation to Fragment Docking. *J. Chem. Inf. Model.* **2019**, *59* (5), 2093−2102.

(12) Kaus, J. W.; Pierce, L. T.; Walker, R. C.; McCammon, J. A. Improving the Efficiency of Free Energy Calculations in the Amber Molecular Dynamics Package. *J. Chem. Theory Comput.* **2013**, *9* (9), 4131.

(13) Lee, T. S.; Allen, B. K.; Giese, T. J.; Guo, Z.; Li, P.; Lin, C.; McGee, T. D., Jr.; Pearlman, D. A.; Radak, B. K.; Tao, Y.; Tsai, H. C.; Xu, H.; Sherman, W.; York, D. M. Alchemical Binding Free Energy Calculations in AMBER20: Advances and Best Practices for Drug Discovery. *J. Chem. Inf. Model.* **2020**, *60* (11), 5595−5623.

(14) Song, L. F.; Lee, T. S.; Zhu, C.; York, D. M.; Merz, K. M. Using AMBER18 for Relative Free Energy Calculations. *J. Chem. Inf. Model.* **2019**, *59* (7), 3128−3135.

(15) Tsai, H. C.; Tao, Y.; Lee, T. S.; Merz, K. M., Jr.; York, D. M. Validation of Free Energy Methods in AMBER. *J. Chem. Inf. Model.* **2020**, *60* (11), 5296−5300.

(16) Hess, B.; Kutzner, C.; van der Spoel, D.; Lindahl, E. GROMACS 4: Algorithms for Highly Efficient, Load-Balanced, and Scalable Molecular Simulation. *J. Chem. Theory Comput.* **2008**, *4* (3), 435−47.

(17) Gapsys, V.; Perez-Benito, L.; Aldeghi, M.; Seeliger, D.; Van Vlijmen, H.; Tresadern, G.; de Groot, B. L. Large scale relative protein ligand binding affinities using non-equilibrium alchemy. *Chem. Sci.* **2020**, *11* (4), 1140−1152.

(18) Brooks, B. R.; Brooks, C. L., 3rd; Mackerell, A. D., Jr.; Nilsson, L.; Petrella, R. J.; Roux, B.; Won, Y.; Archontis, G.; Bartels, C.; Boresch, S.; Caflisch, A.; Caves, L.; Cui, Q.; Dinner, A. R.; Feig, M.; Fischer, S.; Gao, J.; Hodoscek, M.; Im, W.; Kuczera, K.; Lazaridis, T.; Ma, J.; Ovchinnikov, V.; Paci, E.; Pastor, R. W.; Post, C. B.; Pu, J. Z.; Schaefer, M.; Tidor, B.; Venable, R. M.; Woodcock, H. L.; Wu, X.; Yang, W.; York, D. M.; Karplus, M. CHARMM: the biomolecular simulation program. *J. Comput. Chem.* **2009**, *30* (10), 1545−614.

(19) Jung, J.; Mori, T.; Kobayashi, C.; Matsunaga, Y.; Yoda, T.; Feig, M.; Sugita, Y. GENESIS: a hybrid-parallel and multi-scale molecular dynamics simulator with enhanced sampling algorithms for biomolecular and cellular simulations. *Wiley Interdiscip Rev. Comput. Mol. Sci.* **2015**, *5* (4), 310−323.

(20) Cournia, Z.; Allen, B.; Sherman, W. Relative Binding Free Energy Calculations in Drug Discovery: Recent Advances and Practical Considerations. *J. Chem. Inf. Model.* **2017**, *57* (12), 2911−2937.

(21) Cappel, D.; Hall, M. L.; Lenselink, E. B.; Beuming, T.; Qi, J.; Bradner, J.; Sherman, W. Relative Binding Free Energy Calculations Applied to Protein Homology Models. *J. Chem. Inf. Model.* **2016**, *56* (12), 2388−2400.

(22) Raman, E. P.; Paul, T. J.; Hayes, R. L.; Brooks, C. L. Automated, Accurate, and Scalable Relative Protein-Ligand Binding Free-Energy Calculations Using Lambda Dynamics. *J. Chem. Theory Comput.* **2020**, *16* (12), 7895−7914.

(23) Giese, T. J.; York, D. M. A GPU-Accelerated Parameter Interpolation Thermodynamic Integration Free Energy Method. *J. Chem. Theory Comput.* **2018**, *14* (3), 1564−1582.

(24) Lee, T. S.; Cerutti, D. S.; Mermelstein, D.; Lin, C.; LeGrand, S.; Giese, T. J.; Roitberg, A.; Case, D. A.; Walker, R. C.; York, D. M. GPU-Accelerated Molecular Dynamics and Free Energy Methods in Amber18: Performance Enhancements and New Features. *J. Chem. Inf. Model.* **2018**, *58* (10), 2043−2050.

(25) Lee, T. S.; Hu, Y.; Sherborne, B.; Guo, Z.; York, D. M. Toward Fast and Accurate Binding Affinity Prediction with pmemdGTI: An Efficient Implementation of GPU-Accelerated Thermodynamic Integration. *J. Chem. Theory Comput.* **2017**, *13* (7), 3077−3084.

(26) Jo, S.; Kim, T.; Iyer, V. G.; Im, W. CHARMM-GUI: a web-based graphical user interface for CHARMM. *J. Comput. Chem.* **2008**, *29* (11), 1859−65.

(27) Park, S. J.; Lee, J.; Qi, Y. F.; Kern, N. R.; Lee, H. S.; Jo, S.; Joung, I.; Joo, K.; Lee, J.; Im, W. CHARMM-GUI Glycan Modeler for modeling and simulation of carbohydrates and glycoconjugates. *Glycobiology* **2019**, *29* (4), 320−331.

(28) Qi, Y. F.; Lee, J.; Klauda, J. B.; Im, W. CHARMM-GUI Nanodisc Builder for modeling and simulation of various nanodisc systems. *J. Comput. Chem.* **2019**, *40* (7), 893−899.

(29) Lee, J.; Patel, D. S.; Stahle, J.; Park, S. J.; Kern, N. R.; Kim, S.; Lee, J.; Cheng, X.; Valvano, M. A.; Holst, O.; Knirel, Y. A.; Qi, Y. F.; Jo, S.; Klauda, J. B.; Widmalm, G.; Im, W. CHARMM-GUI Membrane Builder for Complex Biological Membrane Simulations with Glycolipids and Lipoglycans. *J. Chem. Theory Comput.* **2019**, *15* (1), 775−786.

(30) Kim, S.; Lee, J.; Jo, S.; Brooks, C. L.; Lee, H. S.; Im, W. CHARMM-GUI ligand reader and modeler for CHARMM force field generation of small molecules. *J. Comput. Chem.* **2017**, *38* (21), 1879−1886.

(31) Hsu, P.-C.; Bruininks, B. M. H.; Jefferies, D.; Cesar Telles de Souza, P.; Lee, J.; Patel, D. S.; Marrink, S. J.; Qi, Y.; Khalid, S.; Im, W. CHARMM-GUI Martini Maker for modeling and simulation of complex bacterial membranes with lipopolysaccharides. *J. Comput. Chem.* **2017**, *38* (27), 2354−2363.

(32) Wu, E. L.; Cheng, X.; Jo, S.; Rui, H.; Song, K. C.; Davila-Contreras, E. M.; Qi, Y.; Lee, J.; Monje-Galvan, V.; Venable, R. M.; Klauda, J. B.; Im, W. CHARMM-GUI Membrane Builder toward realistic biological membrane simulations. *J. Comput. Chem.* **2014**, *35* (27), 1997−2004.

(33) Cheng, X.; Jo, S.; Lee, H. S.; Klauda, J. B.; Im, W. CHARMM-GUI micelle builder for pure/mixed micelle and protein/micelle complex systems. *J. Chem. Inf. Model.* **2013**, *53* (8), 2171−80.

(34) Jo, S.; Kim, T.; Im, W. Automated builder and database of protein/membrane complexes for molecular dynamics simulations. *PLoS One* **2007**, *2* (9), No. e880.

(35) Jo, S.; Lim, J. B.; Klauda, J. B.; Im, W. CHARMM-GUI Membrane Builder for mixed bilayers and its application to yeast membranes. *Biophys. J.* **2009**, *97* (1), 50−8.
(36) Park, S. J.; Lee, J.; Patel, D. S.; Ma, H. J.; Lee, H. S.; Jo, S.; Im, W. Glycan Reader is improved to recognize most sugar types and chemical modifications in the Protein Data Bank. *Bioinformatics* **2017**, *33* (19), 3051−3057.
(37) Lee, J.; Cheng, X.; Jo, S.; MacKerell, A. D.; Klauda, J. B.; Im, W. CHARMM-GUI Input Generator for NAMD, Gromacs, Amber, Openmm, and CHARMM/OpenMM Simulations using the CHARMM36 Additive Force Field. *Biophys. J.* **2016**, *110* (3), 641a−641a.
(38) Lee, J.; Hitzenberger, M.; Rieger, M.; Kern, N. R.; Zacharias, M.; Im, W. CHARMM-GUI supports the Amber force fields. *J. Chem. Phys.* **2020**, *153* (3), 035103.
(39) Kim, S.; Oshima, H.; Zhang, H.; Kern, N. R.; Re, S.; Lee, J.; Roux, B.; Sugita, Y.; Jiang, W.; Im, W. CHARMM-GUI Free Energy Calculator for Absolute and Relative Ligand Solvation and Binding Free Energy Simulations. *J. Chem. Theory Comput.* **2020**, *16* (11), 7207−7218.
(40) Jo, S.; Jiang, W.; Lee, H. S.; Roux, B.; Im, W. CHARMM-GUI Ligand Binder for absolute binding free energy calculations and its application. *J. Chem. Inf. Model.* **2013**, *53* (1), 267−77.
(41) Hopkins, C. W.; Le Grand, S.; Walker, R. C.; Roitberg, A. E. Long-Time-Step Molecular Dynamics through Hydrogen Mass Repartitioning. *J. Chem. Theory Comput.* **2015**, *11* (4), 1864−1874.
(42) Gao, Y.; Lee, J.; Smith, I. P. S.; Lee, H.; Kim, S.; Qi, Y. F.; Klauda, J. B.; Widmalm, G.; Khalid, S.; Im, W. CHARMM-GUI Supports Hydrogen Mass Repartitioning and Different Protonation States of Phosphates in Lipopolysaccharides. *J. Chem. Inf. Model.* **2021**, *61* (2), 831−839.
(43) Loeffler, H. H.; Bosisio, S.; Duarte Ramos Matos, G.; Suh, D.; Roux, B.; Mobley, D. L.; Michel, J. Reproducibility of Free Energy Calculations across Different Molecular Simulation Software Packages. *J. Chem. Theory Comput.* **2018**, *14* (11), 5567−5582.
(44) Steinbrecher, T.; Joung, I.; Case, D. A. Soft-core potentials in thermodynamic integration: comparing one- and two-step transformations. *J. Comput. Chem.* **2011**, *32* (15), 3253−63.
(45) Maier, J. A.; Martinez, C.; Kasavajhala, K.; Wickstrom, L.; Hauser, K. E.; Simmerling, C. ff14SB: Improving the Accuracy of Protein Side Chain and Backbone Parameters from ff99SB. *J. Chem. Theory Comput.* **2015**, *11* (8), 3696−713.
(46) Tian, C.; Kasavajhala, K.; Belfon, K. A. A.; Raguette, L.; Huang, H.; Migues, A. N.; Bickel, J.; Wang, Y.; Pincay, J.; Wu, Q.; Simmerling, C. ff19SB: Amino-Acid-Specific Protein Backbone Parameters Trained against Quantum Mechanics Energy Surfaces in Solution. *J. Chem. Theory Comput.* **2020**, *16* (1), 528−552.
(47) Wang, J.; Wolf, R. M.; Caldwell, J. W.; Kollman, P. A.; Case, D. A. Development and testing of a general amber force field. *J. Comput. Chem.* **2004**, *25* (9), 1157−74.
(48) He, X.; Man, V. H.; Yang, W.; Lee, T. S.; Wang, J. A fast and high-quality charge model for the next generation general AMBER force field. *J. Chem. Phys.* **2020**, *153* (11), 114502.
(49) Jorgensen, W. L.; Chandrasekhar, J.; Madura, J. D.; Impey, R. W.; Klein, M. L. Comparison of Simple Potential Functions for Simulating Liquid Water. *J. Chem. Phys.* **1983**, *79* (2), 926−935.
(50) Horn, H. W.; Swope, W. C.; Pitera, J. W.; Madura, J. D.; Dick, T. J.; Hura, G. L.; Head-Gordon, T. Development of an improved four-site water model for biomolecular simulations: TIP4P-Ew. *J. Chem. Phys.* **2004**, *120* (20), 9665−9678.
(51) Piana, S.; Donchev, A. G.; Robustelli, P.; Shaw, D. E. Water Dispersion Interactions Strongly Influence Simulated Structural Properties of Disordered Protein States. *J. Phys. Chem. B* **2015**, *119* (16), 5113−5123.
(52) Izadi, S.; Anandakrishnan, R.; Onufriev, A. V. Building Water Models: A Different Approach. *J. Phys. Chem. Lett.* **2014**, *5* (21), 3863−3871.
(53) Cumming, J. N.; Smith, E. M.; Wang, L.; Misiaszek, J.; Durkin, J.; Pan, J.; Iserloh, U.; Wu, Y.; Zhu, Z.; Strickland, C.; Voigt, J.; Chen, X.; Kennedy, M. E.; Kuvelkar, R.; Hyde, L. A.; Cox, K.; Favreau, L.; Czarniecki, M. F.; Greenlee, W. J.; McKittrick, B. A.; Parker, E. M.; Stamford, A. W. Structure based design of iminohydantoin BACE1 inhibitors: identification of an orally available, centrally active BACE1 inhibitor. *Bioorg. Med. Chem. Lett.* **2012**, *22* (7), 2444−9.
(54) Wang, L.; Wu, Y.; Deng, Y.; Kim, B.; Pierce, L.; Krilov, G.; Lupyan, D.; Robinson, S.; Dahlgren, M. K.; Greenwood, J.; Romero, D. L.; Masse, C.; Knight, J. L.; Steinbrecher, T.; Beuming, T.; Damm, W.; Harder, E.; Sherman, W.; Brewer, M.; Wester, R.; Murcko, M.; Frye, L.; Farid, R.; Lin, T.; Mobley, D. L.; Jorgensen, W. L.; Berne, B. J.; Friesner, R. A.; Abel, R. Accurate and reliable prediction of relative ligand binding potency in prospective drug discovery by way of a modern free-energy calculation protocol and force field. *J. Am. Chem. Soc.* **2015**, *137* (7), 2695−703.
(55) Raymond, J. W.; Willett, P. Maximum common subgraph isomorphism algorithms for the matching of chemical structures. *J. Comput.-Aided Mol. Des.* **2002**, *16* (7), 521−33.
(56) Dalke, A.; Hastings, J. FMCS: a novel algorithm for the multiple MCS problem. *J. Cheminf.* **2013**, *5*, O6 DOI: 10.1186/1758-2946-5-S1-O6.
(57) Darden, T.; York, D.; Pedersen, L. Particle Mesh Ewald - an N. Log(N) Method for Ewald Sums in Large Systems. *J. Chem. Phys.* **1993**, *98* (12), 10089−10092.
(58) Essmann, U.; Perera, L.; Berkowitz, M. L.; Darden, T.; Lee, H.; Pedersen, L. G. A Smooth Particle Mesh Ewald Method. *J. Chem. Phys.* **1995**, *103* (19), 8577−8593.
(59) Wang, L. L.; Deng, Y. Q.; Knight, J. L.; Wu, Y. J.; Kim, B.; Sherman, W.; Shelley, J. C.; Lin, T.; Abel, R. Modeling Local Structural Rearrangements Using FEP/REST: Application to Relative Binding Affinity Predictions of CDK2 Inhibitors. *J. Chem. Theory Comput.* **2013**, *9* (2), 1282−1293.